JOURNAL OF SYNCHROTRON RADIATION
ISSN 1600-5775

In situ structural studies during denaturation of natural and synthetically crosslinked collagen using synchrotron SAXS

Yi Zhang,[a] Jenna Buchanan,[a] Rafea Naffa,[a] Bradley Mansel,[b] Catherine Maidment,[a] Geoff Holmes[a] and Sujay Prabakar[a]*

[a]Leather and Shoe Research Association of New Zealand, PO Box 8094, Palmerston North 4446, New Zealand, and [b]Chemical Engineering Building, National Tsing Hua University, No. 101, Section 2, Guangfu Road, East District, Hsinchu City 300, Taiwan. *Correspondence e-mail: sujay.prabakar@lasra.co.nz

Received 8 July 2020
Accepted 11 July 2020

Edited by U. Jeng, NSRRC, Taiwan

Keywords: *in situ* SAXS; collagen structure; crosslinks; denaturation.

Supporting information: this article has supporting information at journals.iucr.org/s

Collagen is an important biomacromolecule, making up the majority of the extracellular matrix in animal tissues. Naturally occurring crosslinks in collagen stabilize its intermolecular structure *in vivo*, whereas chemical treatments for introducing synthetic crosslinks are often carried out *ex vivo* to improve the physical properties or heat stability of the collagen fibres for applications in biomaterials or leather production. Effective protection of intrinsic natural crosslinks as well as allowing them to contribute to collagen stability together with synthetic crosslinks can reduce the need for chemical treatments. However, the contribution of these natural crosslinks to the heat stability of collagen fibres, especially in the presence of synthetic crosslinks, is as yet unknown. Using synchrotron small-angle X-ray scattering, the *in situ* role of natural and synthetic crosslinks on the stabilization of the intermolecular structure of collagen in skins was studied. The results showed that, although natural crosslinks affected the denaturation temperature of collagen, they were largely weakened when crosslinked using chromium sulfate. The development of synergistic crosslinking chemistries could help retain the intrinsic chemical and physical properties of collagen-based biological materials.

1. Introduction

During the assembly of collagen molecules to fibrils *in vivo*, enzymatic crosslinking is known to affect the mechanical properties of biological tissues by preventing the slippage of molecules under load (Lucero & Kagan, 2006). The crosslinking is induced by lysyl oxidase which deaminates the ε-amino groups of telopeptidyl lysine and hydroxylysine residues to form aldehydes (Knott & Bailey, 1998). These aldehydes then form Schiff base linkages by condensing with lysine or hydroxylysine residues in the helical region of adjacent collagen molecules (Knott & Bailey, 1998). To date, five types of crosslinks have been identified in bovine skins (Avery & Bailey, 2008; Naffa *et al.*, 2016), *i.e.* divalent dehydro-hydroxylysinonorleucine (deH-HLNL) and dehydro-dihydroxylysinonorleucine (deH-DHLNL), trivalent crosslinked pyridinoline (Pyr) and histidinohydroxylysinonorleucine (HHL), and tetravalent crosslinked dehydro-histidinohydroxymerodesmosine (deH-HHMD), although its presence *in vivo* is disputed (Naffa *et al.*, 2019; Avery & Bailey, 2008). However, amongst these five crosslinks, deH-HLNL, deH-DHLNL and deH-HHMD contain a C=N bond and are labile to acidic conditions (Avery & Bailey, 2008). The chemical modification of hides and skins during leather processing or even collagen extraction can lead to a loss of labile crosslinks, lessening their intrinsic mechanical and heat stability (Avery & Bailey, 2008).

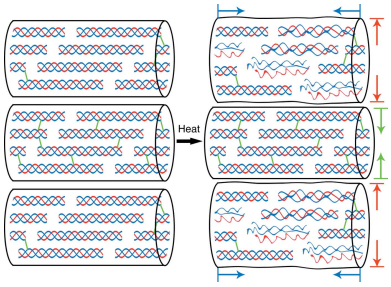

Synthetic crosslinkers are often introduced after the removal of intrinsic crosslinks to stabilize collagen and modify its structure as required (Ashwin & McDonnell, 2010). The mechanism by which synthetic crosslinkers cause an increment in the heat stability of collagen can be explained by the dehydration of the collagen fibres (Miles *et al.*, 2005). Chromium sulfate can covalently bind to the carboxylate groups in collagen and, potentially, form linkages in the collagen matrix (Covington, 2009). It is commonly used to convert animal skins to leather by imparting the material with a higher denaturation temperature and characteristic organoleptic properties (Covington, 2009). However, stringent environmental legislations and increasing pressure by regulatory agencies on the disposal of chromium wastes have led researchers to use less chrome or develop chrome-free alternatives (Lyu *et al.*, 2018; Beghetto *et al.*, 2019; Zhou *et al.*, 2018; Ding *et al.*, 2019). Similarly, biomaterials stabilized by synthetic crosslinkers such as glutaraldehyde can improve the denaturation temperature and protect against enzymatic degradation (Damink *et al.*, 1995; Yang *et al.*, 2017; Skopinska-Wisniewska *et al.*, 2016), although there is the potential to liberate toxic aldehydes during the degradation process (Eybl *et al.*, 1989). By retaining the natural crosslinks that are formed *in vivo* to contribute to the collagen heat stability, the need for additional crosslinking reagents *ex vivo* can be reduced.

Using sodium borohydride, the C═N bonds in acid-labile natural crosslinks can be reduced and stabilized (Eyre *et al.*, 1984). However, it is essential to understand the interplay between natural and synthetic crosslinks and their contribution to the heat stability of collagen structure, which still remains unclear. Using synchrotron-based small-angle X-ray scattering (SAXS), changes in the collagen structure during crosslinking and denaturation can be monitored *in situ* (Buchanan *et al.*, 2019). Also, liquid chromatography–mass spectrometry (LC–MS) can be used to quantify the natural crosslinks present in skin collagen (Naffa *et al.*, 2016). In this work, we studied the effect of natural and synthetic crosslinks on the stability of collagen using a combination of *in situ* synchrotron SAXS and differential scanning calorimetry (DSC).

2. Materials and methods

2.1. Materials and sample preparation

Raw bovine skins were obtained from a local tannery in New Zealand. Commercial reagents including sodium borohydride, sodium hydrosulfide, sodium sulfide, calcium hydroxide, ammonium chloride, hydrogen peroxide, sulfuric acid, sodium chloride, magnesium oxide and Chromosal B (25% Cr_2O_3, 33% basicity) were used without further modification.

Raw bovine skins were treated with 3 wt% (wt% of the skin, same below) sodium borohydride at 25°C for 24 h, termed 'reduced control (R-CT)', whereas the negative controls without borohydride treatment were termed 'non-reduced control (N-CT)'. The skins were then treated overnight at 25°C in a solution of 2.5 wt% sodium sulfide, 1.5 wt% sodium hydrosulfide and 1.5 wt% calcium hydroxide and rinsed with water to remove hair. Then, the skins were neutralized with a solution of 2.5 wt% ammonium chloride and 0.5 wt% hydrogen peroxide for 2 h, followed by rinsing with water. Samples collected at this stage are termed 'dehaired' (N-DH and R-DH). The skins were then acidified using 1.2 wt% sulfuric acid with 8 wt% sodium chloride to pH = 3.0, followed by sample collection as 'acidified' (N-AC and R-AC). Finally, the skins were treated using 8 wt% chromium sulfate overnight at 25°C, followed by the addition of 0.4 wt% magnesium oxide to adjust the pH to 4.0, termed 'crosslinked' (N-CR and R-CR). All samples were kept at 4°C prior to further analysis.

2.2. *In situ* SAXS analysis

In situ isotropic SAXS measurements were performed on beamline 23A1 at the National Synchrotron Radiation Research Centre (NSRRC) in Hsinchu, Taiwan. Experiments were carried out in the standard beamline temperature-controlled cell with the X-ray beam perpendicular to the skin surface. Samples 0.5 cm × 0.5 cm × 1 mm ($L \times W \times H$) in size were cut out and loaded onto the cell and sealed in polyimide film to prevent sample dehydration. Measurements of 30 s with an energy of 15 keV were performed. Scattered radiation was collected using a Pilatus 1M detector located at a distance of 3.233 m from the sample.

The scattered intensity $I(q)$ is presented as a function of scattering vector q, with $q = 4\pi \sin(\theta/2)/\lambda$, where θ is the angle between the incident and scattered radiation. The acquired SAXS scattering patterns were radially integrated into 1D plots, and the diffraction peaks were fitted to calculate the d-spacing following a previously reported approach (Zhang *et al.*, 2018; Ingham *et al.*, 2009). The diffraction peaks are modelled as Gaussians,

$$I_{\text{peaks}}(q) = \sum_n \frac{A_n}{w(q)(\pi/2)^{1/2}} \exp\left\{\frac{-2[q-(2\pi n/d)]^2}{w(q)^2}\right\},$$

where A_n is the area of peak n, d is the D-period (in Å), and $w(q)$ is the width, expressed as $w(q) = a + bq$ where a and b are fitted parameters. During the temperature increase, the onset temperatures of D-period (T_{onset}) are calculated to indicate the beginning of structural events.

2.3. LC–MS analysis

Natural crosslinks of bovine skins were analysed based on a previously reported method (Naffa *et al.*, 2016), using a Cogent Diamond Hydride HPLC column (150 mm × 2.1 mm, particle size 2.2 µm, pore size 100 Å; Microsolv Technology, Leland, NC, USA) and Q-Exactive hybrid quadrupole-orbitrap high-resolution accurate-mass spectrometry (Thermo Fisher Scientific, San Jose, USA). In brief, lyophilized skins were weighed and rehydrated in a phosphate buffered saline then reduced with sodium borohydride at 25°C for 24 h. The reduction was quenched by adjusting the pH to 3.0 using acetic acid, and then the reduced samples were washed three times

with water and lyophilized. The lyophilized reduced samples were hydrolysed in 3 ml of 6 *M* HCl containing 3% phenol at 105°C for 24 h and the resulting hydrolysates were then dried and rehydrated in 1 ml of water. A volume of 10 µl was removed from each sample for the analysis of hydroxyproline content in order to estimate the collagen content in skin based on previous work (Kliment *et al.*, 2011). The remaining samples were subjected to a CF-11 column and the water eluent containing the crosslinks was then lyophilized and dissolved in 1 ml of water. The total concentration of natural crosslinks was determined and normalized with respect to the collagen content of the sample.

2.4. DSC analysis

DSC measurements were carried out using a Q2000 calorimeter (TA Instruments). Lyophilized samples were rehydrated overnight with deionized water of the same weight and then encapsulated in hermetically sealed aluminium pans (10 µl). All measurements were carried out over the temperature range from 30°C to 120°C under N_2 purge and at a heating rate of 5°C min^{-1}. The onset temperatures of the heat flow curve (T_d) were marked to highlight the starting point of the thermal events.

3. Results and discussion

3.1. Quantitative analysis of the natural crosslinks: LC–MS

The reduction of C═N to CH—NH [Fig. 1(*a*)] is known to stabilize natural crosslinks from acidic degradation (Eyre *et al.*, 1984). The quantity of natural crosslinks was analysed using LC–MS showing the variation across the eight groups of samples [Fig. 1(*b*)] (see Section 2.1 for differences in sample preparation). From control (CT) to dehaired (DH), natural crosslinks remain unchanged for both reduced and non-reduced skin samples (N-CT, R-CT, N-DH and R-DH) owing to the mild pH conditions (pH = 8). When skin samples were acidified (AC) to pH = 3, the number of total crosslinks decreased in the non-reduced samples (N-AC), whereas no change was observed for the reduced samples (R-AC). This is direct evidence of the completed reduction of labile crosslinks in the reduced skin, which makes the labile crosslinks stable under acidic conditions. Interestingly, after synthetic cross-linking using chromium sulfate, the detected amounts of natural crosslinks decrease for both reduced and non-reduced samples (N-CR and R-CR). A detrimental effect of chromium on natural crosslinks was previously reported in ovine skins (Zhang *et al.*, 2018), which can also explain our observation here in bovine skins.

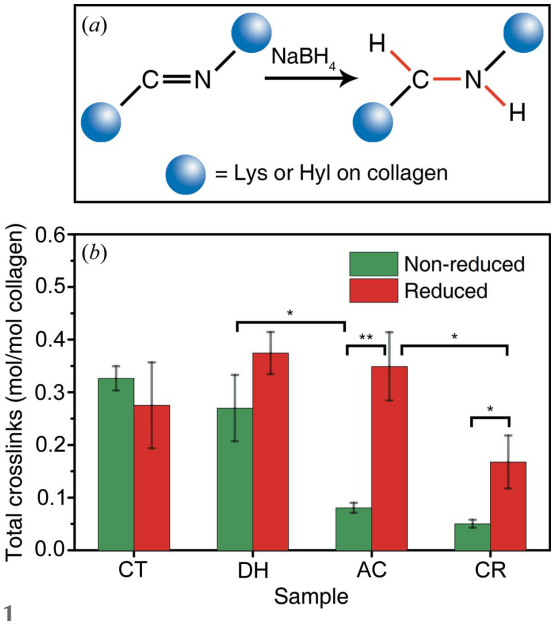

Figure 1
(*a*) Schematic representation of the reduction of natural crosslinks by $NaBH_4$. (*b*) Total number of natural crosslinks in reduced and non-reduced bovine skin samples (CT = control, DH = dehaired, AC = acidified, CR = crosslinked). The quantity of each individual natural crosslink is shown in the supporting information. Statistically significant changes between samples are highlighted using asterisks (* for $p < 0.05$, ** for $p < 0.01$).

3.2. Effect of natural and synthetic crosslinks on collagen structure during denaturation: *in situ* SAXS

In situ monitoring of the structural changes during collagen denaturation was conducted using SAXS. Typical SAXS 2D patterns of collagen were observed [Fig. 2(*a*) shows a pattern of an N-CR sample] and a 1D profile is displayed for each type of sample [Fig. 2(*b*)]. The increase in overall peak intensity confirmed the synthetic crosslinking effect by chromium sulfate, in agreement with previous reports (Buchanan *et al.*, 2019). The intermolecular packing of collagen follows a quarter-staggered arrangement, resulting in a gap and overlap banding structure with a characteristic periodicity in the axial direction (*D*-period) (Petruska & Hodge, 1964). When collagen denatures under moist heat, the triple helix uncoils and the intermolecular structure in the collagen fibril loses the long-range order as well as collapsing in the axial direction, as depicted in Fig. 2(*a*). This leads to a diminished intensity of the diffraction rings on the SAXS pattern [Figs. 2(*a*) and S3] and a decreased *D*-period [Figs. 2(*f*)–2(*m*)] (Zhang *et al.*, 2018). However, in this study, R-CT and N-CT [Figs. 2(*f*) and 2(*j*)] showed unchanged *D*-periods during denaturation, whereas the other samples [Figs. 2(*g*)–2(*i*) and 2(*k*)–2(*m*)] showed clear decreasing trends. The unchanged *D*-period in CT samples during denaturation could be attributed to the non-covalent binding of inter-fibrillary non-collagenous proteins such as dermatan sulfate which constrains the collagen structure (Stinson & Sweeny, 1980). These proteins are removed during dehairing (Covington, 2009), thereby enabling the changes in *D*-period when denaturation occurs. Interestingly, the propensity of collagen fibrils to shrink in the axial direction due to the uncoiling of collagen molecules during denaturation is not suppressed by the presence of natural crosslinks. When the collagen triple helix uncoils during denaturation, steric hindrance due to the binding of collagen with non-collagenous proteins in the helical region could play a more important role than the constraining force by natural cross-links in the telopeptidyl region.

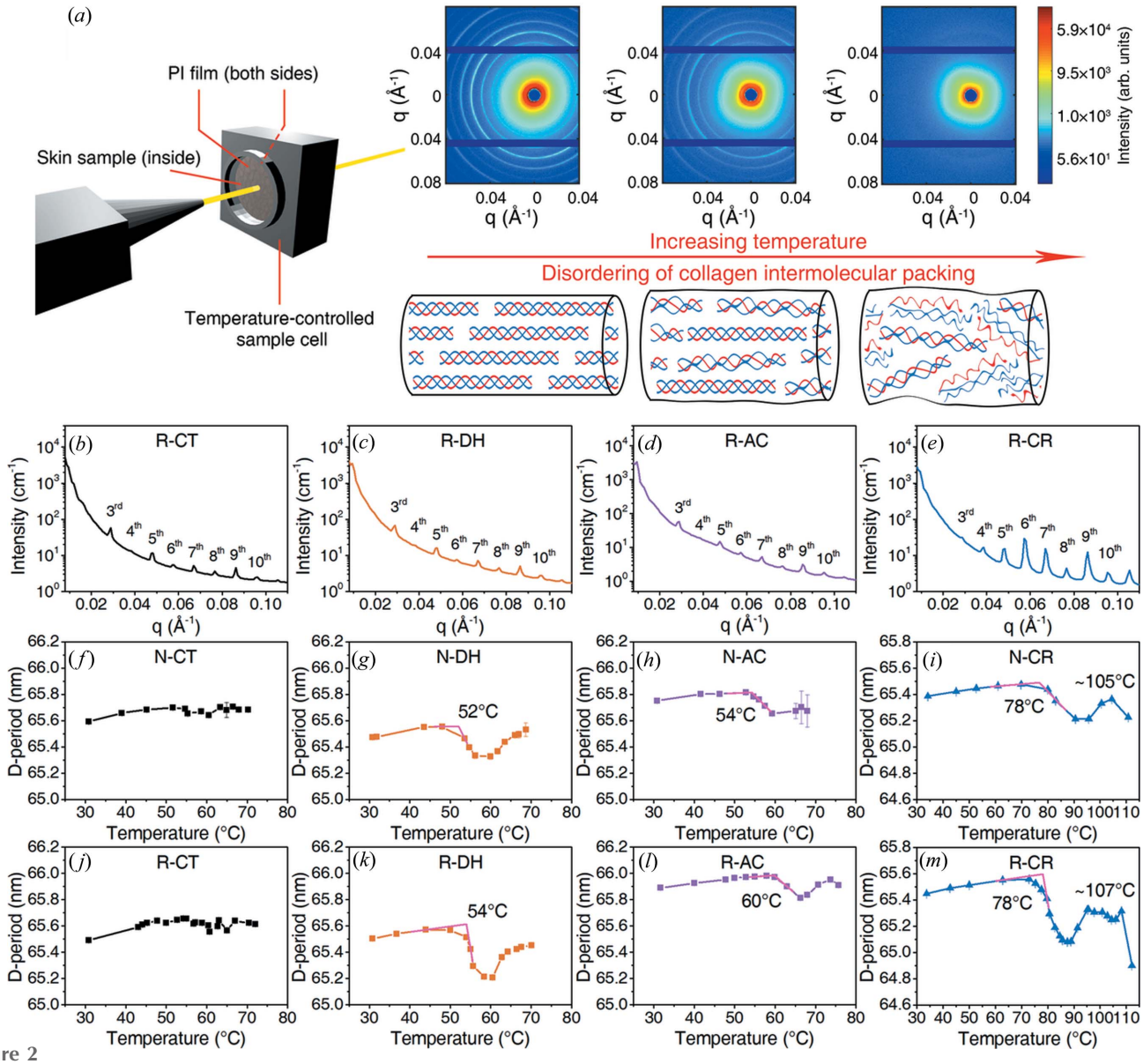

Figure 2

(*a*) Experimental setup of *in situ* SAXS measurements and the 2D SAXS pattern from sample N-CR (corresponding 1D plots shown in Fig. S3), showing changes during the uncoiling of the collagen triple helix and the disordering of its intermolecular structure in the fibrils when temperature increases. (*b*)–(*e*) Radially integrated 1D SAXS profiles of reduced collagen samples to highlight peak intensity changes. (*f*)–(*m*) Changes in *D*-period obtained from *in situ* SAXS data analysis during heat denaturation of the collagen in bovine skins [N = non-reduced, R = reduced, CT = control (pH = 8), DH = dehaired (pH = 8), AC = acidified (pH = 3), CR = crosslinked (pH = 4)]. The onset temperatures (T_{onset}) of the *D*-period during denaturation are calculated and labelled alongside each curve.

The onset temperature of *D*-period (T_{onset}) for N-DH (52°C) was similar to that of R-DH (54°C) [Figs. 2(*g*) and 2(*k*)]. After acidification, the T_{onset} increased to 54°C in N-AC and 60°C in R-AC [Figs. 2(*h*) and 2(*l*)]. To prevent damage to the fibril structure caused by swelling at pH = 3, sodium chloride was added along with the sulfuric acid, which can result in reduced intermolecular hydration and a slight increase in T_{onset}. Also, T_{onset} was higher by 6°C in the reduced sample R-AC (60°C) than in the non-reduced sample N-AC (54°C). The difference in T_{onset} matches with the greater concentration of natural crosslinks in R-AC than N-AC. We speculate that retained natural crosslinks result in a dehydration effect in the collagen fibres, leading to denser packing of collagen molecules, reducing their entropy thereby increasing the heat stability (Miles & Ghelashvili, 1999; Miles *et al.*, 2005).

When acidified skins are synthetically crosslinked using an excess of chromium sulfate, both N-CR and R-CR show similar T_{onset} at 78°C [Figs. 2(*i*) and 2(*m*)]. When both natural and synthetic crosslinks are presented in the collagen matrix, the denaturation temperature of collagen is determined by the labile domains in its triple helix with relatively less steric hindrance and a lower activation energy required for the polypeptide chains to uncoil (Miles & Bailey, 2001). Our results suggest that the contribution to the activation energy required for the uncoiling of the collagen triple helix from

synthetic crosslinks is much higher than the retained natural crosslinks. Therefore, in our case, the T_{onset} of the collagen molecule is dominated by the contribution of the synthetic crosslinks. We also observe a second peak around 105°C in both N-CR and R-CR [Figs. 2(*i*) and 2(*m*)]. In our previous work, we suggested two mechanisms during the uncoiling of the collagen triple helix when crosslinked using chromium sulfate (Zhang *et al.*, 2018) and these are further confirmed by the results in this study. The first T_{onset} at 78°C can be assigned to the conformational changes in the thermally labile domains in collagen molecules due to the covalent crosslinking with chromium sulfate. The second peak can be attributed to the complete uncoiling of collagen triple helices to random coils and the disordering of the intermolecular structure of collagen in the fibrils due to non-covalent interactions with chromium sulfate when an excess is used to crosslink the collagen.

A common feature was also observed in DH, AC and CR samples where the *D*-period showed an initial decrease followed by an increase after the first T_{onset} peak [Figs. 2(*g*)–2(*i*) and 2(*k*)–2(*m*)]. This could be caused by the presence of two populations of fibrils during heating, one remains intact and the other becomes denatured (Fig. 3). When the temperature reaches T_{onset} of a skin sample, the thermally unstable collagen molecules in the fibrils start to uncoil (Fig. 3). During uncoiling, the axial packing of the collagen molecules becomes denser (decrease in *D*-period), accompanied by swelling in the lateral direction of the fibrils as previously reported (Zhang *et al.*, 2018). However, at T_{onset} the other population of collagen fibrils remains intact with the original *D*-period. As the temperature increases the overall peak intensity is reduced due to the intensity decrease from the denaturing population and the unchanged intensity from the intact population (Fig. S2 of the supporting information). Therefore, it is observed as the combination of diffraction signal from (i) intact collagen fibrils, with unchanged *D*-period and intensity, and (ii) denaturing collagen fibrils, showing a decrease in both *D*-period and intensity. When the intermolecular structure of the denaturing population is partially disordered, the peak intensities from both populations are comparable. When the diffraction peaks combine, we observe a shift in the peak towards lower *D*-period. When the denaturing fibrils are completely denatured, the observed intensity arises only from the intact fibrils, albeit weakly (Fig. S4). The presence of the two populations (intact and denaturing) can be explained on the basis of structural constraints. Miles & Ghelashvili (1999) previously reported an increase in the heat stability of the collagen triple helix from structural constraints due to the denser packing of the collagen molecules in the fibrils. Structural constraints may be caused by high crosslink density in the intact population of fibrils, or from swelling of the denaturing fibrils adjacent to the intact ones during temperature ramp (Fig. 3).

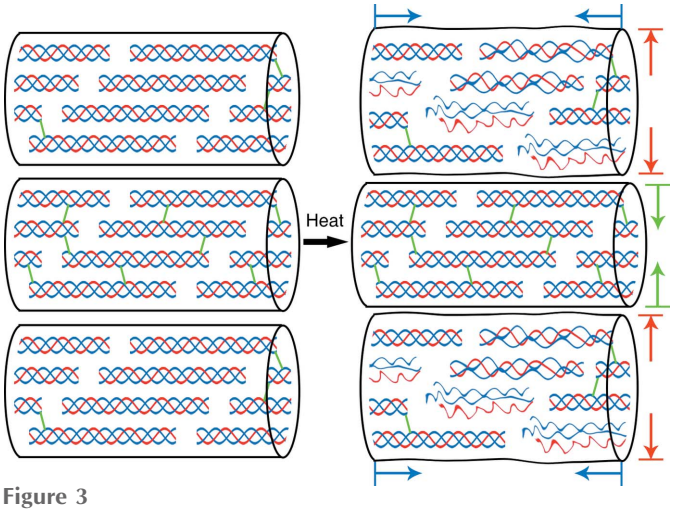

Figure 3
Schematic of the changes in the collagen triple helices and the intermolecular structure in collagen fibrils when temperature increases. Two populations of fibrils are shown: (i) intact collagen fibrils, with unchanged axial packing under heat, and (ii) denaturing collagen fibrils, showing a decrease in the axial packing distance (blue arrows) and swelling in the lateral direction during thermal denaturation (red arrows). The high density of crosslinks (green links) between the collagen molecules of the intact fibrils, or the compression in the lateral direction (green arrows) caused by the swelling of adjacent fibrils, could contribute to the increase in structural constraint and heat stability.

3.3. Effect of natural and synthetic crosslinks on the denaturation temperature of collagen: DSC

DSC results (Fig. 4) from the denaturation of collagen were generally in agreement with the *in situ* SAXS analyses. The denaturation temperatures (T_d) of N-CT and R-CT were both 64°C but decrease to 54°C and 56°C for N-DH and R-DH, possibly due to the removal of non-collagenous proteins. When acidified, a T_d difference of 4°C was observed for N-AC (55°C) and R-AC (59°C), confirming the contribution of natural crosslinks to the heat stability of collagen. However, in the crosslinked samples (N-CR and R-CR), DSC results show

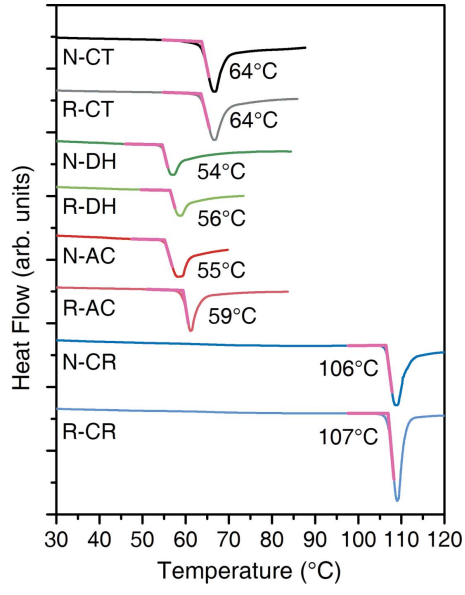

Figure 4
DSC results of reduced and non-reduced bovine skins (N = non-reduced, R = reduced, CT = control, DH = dehaired, AC = acidified, CR = crosslinked). The denaturation temperatures (T_d) of each sample are calculated and labelled alongside each curve.

a single peak instead of two as shown in Figs. 2(*i*) and 2(*m*). The T_d of both crosslinked samples (106°C and 107°C) match the second peak in the SAXS plots [∼105°C and ∼107°C, Figs. 2(*i*) and 2(*m*)], whereas no changes in heat flow were observed at temperatures around the first T_{onset} found in SAXS (78°C). Based on these observations, we suggest that: (i) the changes in collagen *D*-period at 78°C are driven by the entropy changes during the conformational changes in the collagen molecules, which involve only minor enthalpy changes, (ii) the complete uncoiling of collagen triple helices to random coils above 100°C involves both significant enthalpy changes and structural changes. Nevertheless, the effects of retained natural crosslinks on the heat stability of collagen were overwhelmed by the strong chemical binding from chromium sulfate.

4. Conclusions

In summary, natural crosslinks that are formed *in vivo* during collagen assembly can improve the heat stability of collagen molecules, but do not constrain the intermolecular structure to prevent the changes in *D*-period when denatured. However, the quantity of natural crosslinks decreases when chromium sulfate is involved, and their contributions towards the heat stability of the collagen structure are largely overwhelmed by synthetic crosslinks. Further research on the interplay between natural crosslinks and a wide range of synthetic crosslinkers could help retain the intrinsic properties of collagen in biological materials.

Acknowledgements

SP, YZ and BM thank NSRRC for SAXS beam time on the TLS BL23A1 beamline. The authors declare that they have no known competing financial interests or personal relationships that could have appeared to influence the work reported in this paper.

Funding information

The following funding is acknowledged: Ministry of Business, Innovation and Employment, New Zealand (grant No. LSRX-1801).

References

Ashwin, P. T. & McDonnell, P. J. (2010). *Br. J. Ophthalmol.* **94**, 965–970.
Avery, N. & Bailey, A. (2008). *Collagen*, edited by P. Fratzi, pp. 81–110. Boston: Springer.
Beghetto, V., Agostinis, L., Gatto, V., Samiolo, R. & Scrivanti, A. (2019). *J. Clean. Prod.* **220**, 864–872.
Buchanan, J. K., Zhang, Y., Holmes, G., Covington, A. D. & Prabakar, S. (2019). *ChemistrySelect*, **4**, 14091–14102.
Covington, A. D. (2009). *Tanning Chemistry: the Science of Leather.* Cambridge: Royal Society of Chemistry.
Ding, W., Yi, Y., Wang, Y., Zhou, J. & Shi, B. (2019). *Carbohydr. Polym.* **224**, 115–169.
Eybl, E., Griesmacher, A., Grimm, M. & Wolner, E. (1989). *J. Biomed. Mater. Res.* **23**, 1355–1365.
Eyre, D. R., Paz, M. A. & Gallop, P. M. (1984). *Annu. Rev. Biochem.* **53**, 717–748.
Ingham, B., Li, H., Allen, E. L. & Toney, M. F. (2009). arXiv: 0901.4782.
Kliment, C. R., Englert, J. M., Crum, L. P. & Oury, T. D. (2011). *Int. J. Clin. Exp. Pathol.* **4**, 349–355.
Knott, L. & Bailey, A. J. (1998). *Bone*, **22**, 181–187.
Lucero, H. & Kagan, H. (2006). *Cell. Mol. Life Sci.* **63**, 2304–2316.
Lyu, B., Chang, R., Gao, D. & Ma, J. (2018). *ACS Sustain. Chem. Eng.* **6**, 5413–5423.
Miles, C. A., Avery, N. C., Rodin, V. V. & Bailey, A. J. (2005). *J. Mol. Biol.* **346**, 551–556.
Miles, C. & Bailey, A. (2001). *Micron*, **32**, 325–332.
Miles, C. A. & Ghelashvili, M. (1999). *Biophys. J.* **76**, 3243–3252.
Naffa, R., Holmes, G., Ahn, M., Harding, D. & Norris, G. (2016). *J. Chromatogr. A*, **1478**, 60–67.
Naffa, R., Maidment, C., Ahn, M., Ingham, B., Hinkley, S. & Norris, G. (2019). *Int. J. Biol. Macromol.* **128**, 509–520.
Olde Damink, L. H. H., Dijkstra, P. J., Van Luyn, M., Van Wachem, P., Nieuwenhuis, P. & Feijen, J. (1995). *J. Mater. Sci. Mater. Med.* **6**, 460–472.
Petruska, J. A. & Hodge, A. J. (1964). *Proc. Natl Acad. Sci. USA*, **51**, 871–876.
Skopinska-Wisniewska, J., Wegrzynowska-Drzymalska, K., Bajek, A., Maj, M. & Sionkowska, A. (2016). *J. Mater. Sci. Mater. Med.* **27**, 67.
Stinson, R. H. & Sweeny, P. R. (1980). *Biochim. Biophys. Acta*, **621**, 158–161.
Yang, J., Ding, C., Huang, L., Zhang, M. & Chen, L. (2017). *Int. J. Biol. Macromol.* **97**, 1–7.
Zhang, Y., Mansel, B. W., Naffa, R., Cheong, S., Yao, Y., Holmes, G., Chen, H.-L. & Prabakar, S. (2018). *ACS Sustain. Chem. Eng.* **6**, 7096–7104.
Zhou, Y., Ma, J., Gao, D., Li, W., Shi, J. & Ren, H. (2018). *J. Clean. Prod.* **201**, 668–677.